

1 **A virus associated with the zoonotic pathogen *Plasmodium knowlesi***
2 **causing human malaria is a member of a diverse and unclassified viral**
3 **taxon**

4
5 Mary E. Petrone^{1,2*†}, Justine Charon^{3*}, Matthew J Grigg^{4,5}, Timothy William^{5,6}, Giri S
6 Rajahram^{5,7}, Jacob Westaway⁴, Kim A Piera⁴, Mang Shi^{8,9,10,11}, Nicholas M. Anstey^{4,5},
7 Edward C. Holmes^{2,12}

8
9 ¹Sydney Institute for Infectious Diseases, School of Medical Sciences, The University of
10 Sydney, Sydney, NSW 2006, Australia.

11 ²Laboratory of Data Discovery for Health Limited, Hong Kong SAR, China.

12 ³Fruit Biology and Pathology Unit, University of Bordeaux, INRAE, Bordeaux, France

13 ⁴Global and Tropical Health Division, Menzies School of Health Research, Charles Darwin
14 University, Darwin, Australia.

15 ⁵Infectious Diseases Society Kota Kinabalu Sabah - Menzies School of Health Research
16 Clinical Research Unit, Kota Kinabalu, Malaysia.

17 ⁶Subang Jaya Medical Centre, Subang Jaya, Malaysia.

18 ⁷Queen Elizabeth Hospital II, Ministry of Health Malaysia, Kota Kinabalu, Sabah, Malaysia.

19 ⁸State Key Laboratory for Biocontrol, School of Medicine, Shenzhen Campus of Sun Yat-sen
20 University, Sun Yat-sen University, Shenzhen, China.

21 ⁹National Key Laboratory of Intelligent Tracking and Forecasting for Infectious Diseases, Sun
22 Yat-sen University, Shenzhen, China.

23 ¹⁰Shenzhen Key Laboratory for Systems Medicine in Inflammatory Diseases, Shenzhen
24 Campus of Sun Yat-sen University, Sun Yat-sen University, Shenzhen, China.

25 ¹¹Guangdong Provincial Center for Disease Control and Prevention, Guangzhou, China.

26 ¹²School of Medical Sciences, The University of Sydney, Sydney, NSW 2006, Australia.

27
28 *Contributed equally

29 †Correspondence: mary.petrone@sydney.edu.au

30
31
32 **ABSTRACT**

33 Apicomplexa are single-celled eukaryotes that can infect humans and include the mosquito-
34 borne parasite *Plasmodium*, the cause of malaria. Increasing rates of drug resistance in
35 human-only *Plasmodium* species are reducing the efficacy of control efforts and antimalarial
36 treatments. There are also rising cases of *P. knowlesi*, the only zoonotic *Plasmodium* species
37 that causes severe disease and death in humans. Thus, there is a need to develop additional
38 innovative strategies to combat malaria. Viruses that infect non-*Plasmodium* spp. disease-
39 causing protozoa have been shown to affect pathogen life cycle and disease outcomes.
40 However, only one virus (Matryoshka RNA virus 1) has been identified in *Plasmodium*, and
41 none have been identified in zoonotic *Plasmodium* species. The rapid expansion of the known
42 RNA virosphere using structure- and artificial intelligence-based methods suggests that this
43 dearth is due to the divergent nature of RNA viruses that infect protozoa. We leveraged these
44 newly uncovered data sets to explore the virome of human-infecting *Plasmodium* species
45 collected in Sabah, east (Borneo) Malaysia. We identified a highly divergent RNA virus in two

46 human-infecting *P. knowlesi* isolates that is related to the unclassified group ‘ormycoviruses’.
47 By characterising fifteen additional ormycoviruses identified in the transcriptomes of
48 arthropods we show that this group of viruses exhibits a complex ecology at the arthropod-
49 mammal interface. Through the application of artificial intelligence methods, we then
50 demonstrate that the ormycoviruses are part of a diverse and unclassified viral taxon. This is
51 the first observation of an RNA virus in a zoonotic *Plasmodium* species. By linking small-scale
52 experimental data to large-scale virus discovery advances, we characterise the diversity and
53 genomic architecture of an unclassified viral taxon. This approach should be used to further
54 explore the virome of disease-causing Apicomplexa and better understand how protozoa-
55 infecting viruses may affect parasite fitness, pathobiology, and treatment outcomes.

56 57 INTRODUCTION

58 Parasitic protozoa are a highly diverse collection of single-celled eukaryotes that can cause
59 disease in many vertebrates. Organisms belonging to the phylum Apicomplexa are associated
60 with a range of human diseases including malaria (*Plasmodium*), inflammation of the brain
61 (*Toxoplasma*)¹, diarrhea (*Cryptosporidium*)², and severe anaemia (*Babesia*)³. *Plasmodium* is
62 the leading cause of death from Apicomplexa in humans worldwide⁴. This mosquito-borne
63 infection is estimated to have caused over 240 million cases of malaria and to have killed over
64 600,000 people in 2022 alone⁵.

65
66 Efforts to control and treat malaria are challenged by the complex ecology of this parasite⁶ and
67 mounting antimalarial resistance^{7,8}. Of the five human-only infecting species of *Plasmodium*
68 (*P. falciparum*, *P. vivax*, *P. malariae*, *P. ovale wallikeri*, and *P. ovale curtisii*), *P. falciparum* and
69 *P. vivax* cause the greatest morbidity and mortality, with *P. falciparum* accounting for more than
70 95% of malaria fatalities⁴. Partial resistance of *P. falciparum* to artemisinin is entrenched in the
71 Greater Mekong subregion of Southeast Asia^{9,10} and has now emerged independently in
72 Africa^{5,11,8}. Eight additional *Plasmodium* species can cause human malaria through zoonotic
73 transmission via mosquito vectors¹². Among these, *P. knowlesi* is the only species to cause
74 severe disease and death in humans^{4,13-15}. Although predominating in Malaysian Borneo^{16,17},
75 *P. knowlesi* is now recognised as a significant cause of malaria across Southeast Asia¹⁸, in
76 association with changing land use and deforestation¹⁸⁻²¹, and in areas with declining
77 incidence of the cross-protective species, *P. vivax*²². Thus, innovative strategies are needed
78 to combat and control *Plasmodium* as the efficacy of accessible treatments declines in the
79 human-only species, and changes in land-use cause greater numbers of zoonotic malaria
80 cases.

81

82 One potential approach for malaria control involves the use of viruses that infect disease-
83 causing protozoa. In a similar manner to how bacteriophage have been leveraged to combat
84 drug-resistant bacterial infections²³⁻²⁵, protozoa-infecting viruses have been proposed as a
85 potential new avenue for therapeutics^{26,27}. These parasitic protozoan viruses (PPVs)²⁷ have
86 been identified in *Giardia*, *Leishmania*, *Cryptosporidium*^{28,29}, *Eimeria*³⁰⁻³⁸, *Toxoplasma*³⁹, *P.*
87 *vivax*^{40,41}, and *Babesia*^{42,43}. They are of particular interest because some impact the parasite
88 life cycle and modulate disease outcomes in the parasite host. Notably, *Leishmania* species
89 that harbour Leishmania RNA virus 1 have been associated with an increased risk of treatment
90 failure in humans⁴⁴ and more severe disease outcomes in mice⁴⁵. Similarly, it has been
91 proposed that infection of *Toxoplasma* with the recently characterised apocryptoviruses
92 (*Narnaviridae*) may be associated with increased disease severity in humans³⁹, although this
93 has yet to be formally tested. *Cryptosporidium parvum* virus 1 modulates the interferon
94 response in *Cryptosporidium*-infected mammals⁴⁶. To date, however, only one virus,
95 Matryoshka RNA virus 1, has been identified in a *Plasmodium* species (*P. vivax*)^{40,41}, and it is
96 not known whether this virus impacts *Plasmodium* fitness or disease pathogenesis in humans.

97
98 Extending the known diversity of PPVs requires innovative approaches to virus discovery
99 because both protozoa and the viruses that infect them are likely ancient and often highly
100 divergent. As a case in point, the ormycoviruses were first identified in parasitic protozoa and
101 fungi using structure-based methods⁴⁷ and have since been identified in kelp (Stramenopila)⁴⁸,
102 ticks⁴⁹, palm⁵⁰, and additional fungal species^{51,52}. This group of bi-segmented RNA viruses
103 shares no measurable phylogenetic relationship to known viral taxa, rendering it invisible to
104 sequence-based discovery methods⁴⁷. Little else is known about ormycoviruses including their
105 complete host range or whether they encode positive- or negative-sense genomes. The
106 application of artificial intelligence-based methods⁵³, in addition to large-scale sampling of
107 aquatic environments⁵⁴, has further uncovered previously inaccessible virus diversity,
108 including entirely novel “supergroups” of unclassified viral taxa⁵³. These tools and the data
109 they have generated can be leveraged to explore the viromes of disease-causing protozoa
110 including *Plasmodium*.

111
112 In this study, we combine these facets of virus discovery to characterise a divergent virus
113 associated with human-infecting *P. knowlesi* isolates. We contextualise this virus within the
114 vast viral diversity revealed through large-scale virus discovery studies. We also explore the
115 complex ecology of viruses that infect parasites and can be transmitted as passengers to
116 mammalian hosts. Our findings extend the diversity of known *Plasmodium*-associated viruses
117 and highlight the importance of integrating large- and small-scale virus discovery research to
118 better understand viruses that infect these ancient, microscopic hosts.

119

120 RESULTS

121 Identification of a divergent RNA virus associated with human-infecting *Plasmodium* 122 *knowlesi*

123 To extend the known diversity of RNA viruses in disease-causing Apicomplexa, we analysed
124 the metatranscriptomes of 18 human blood samples with PCR-confirmed *Plasmodium*
125 infections and six uninfected human controls, collected in Sabah, east (Borneo) Malaysia
126 between 2013 and 2014. These samples are the same as those previously described⁴⁰. Of the
127 patients with malaria, seven were infected with *P. vivax*, six with *P. knowlesi*, and five with *P.*
128 *falciparum*⁴⁰. Sequencing libraries were pooled according to *Plasmodium* species as were the
129 negative controls, resulting in four libraries (SRR10448859-62, BioProject PRJNA589654).
130 Matryoshka RNA virus 1 was previously found exclusively in all seven *P. vivax* isolates
131 (SRR10448862)⁴⁰.

132

133 We searched each library for divergent viruses using the RdRp-scan bioinformatic pipeline⁵⁵.
134 This revealed a putative, highly divergent RNA-dependent RNA polymerase (RdRp) that was
135 3,177nt in length with a complete open reading frame (ORF) and robust sequencing coverage
136 in the *P. knowlesi* library (SRR10448860) (**Fig. 1a**). No identical or related sequences were
137 found in the other three libraries. The transcript was relatively abundant (1.4% of non-rRNA
138 reads), and we confirmed the presence of this putative RdRp in two of the six isolates in the
139 pool using RT-PCR (**Table S1, Fig. S1**). Both patients with putative virus-infected *P. knowlesi*
140 isolates were from Kota Marudu district residing in villages approximately 30km apart. There
141 was three months difference in the date of hospital presentation. Both had uncomplicated
142 malaria with parasitemia of 7,177 and 41,882 parasites/ μ L, respectively, which were higher
143 than the median parasitemia found in the *P. knowlesi* infections that lacked the putative virus
144 (4,518/ μ L). Parasitemia was correlated with the RdRp signals we observed with PCR (**Fig.**
145 **S1**).

146

147 Further inspection indicated that this putative virus was a bi-segmented ormycovirus likely
148 infecting the *Plasmodium*. The divergent RdRp shared low but detectable similarity with that
149 of seven previously identified viruses, of which six were ormycoviruses (**Table S2**). We
150 identified a putative second segment of unknown function, 1,721nt in length sharing 22.8%
151 identity (e-value = 3.14×10^{-15}) with the hypothetical protein of Erysiphe lesion-associated
152 ormycovirus 1 (USW07196). The structures of the putative and known hypothetical proteins
153 were significantly similar (p-value = 1.62×10^{-2}) when predicted with AlphaFold2^{56,57} and
154 compared by pairwise alignment with FATCAT⁵⁸ (**Fig. 1b**). Similar transcripts were not
155 identified in the ormycovirus-negative libraries from the same BioProject. Analysis of the library

156 composition with CCMetagen⁵⁹ and the KMA database⁶⁰ did not reveal plausible host
157 candidates aside from the *Plasmodium*, which comprised 24% of non-rRNA reads. The
158 remainder aligned to the *Hominidae*, reflecting that the *Plasmodium* were themselves infecting
159 humans. We assumed that the host range of the ormycoviruses likely did not extend to
160 vertebrates, consistent with their absence in the humans without *Plasmodium* infection. Unlike
161 its closest relatives, the *P. knowlesi*-associated RdRp encoded GDD in motif C of its palm
162 domain rather than NDD (**Fig. 1c**).

163

164 To assess the prevalence of this and other ormycoviruses in *P. knowlesi*, we screened 1,470
165 *P. knowlesi* RNA SRA libraries (**Supp. Data 1**) with a custom ormycovirus database. This
166 returned no additional ormycovirus candidates. However, all 1,470 libraries were generated
167 from only seven BioProjects, and only the library we generated was derived from human-host
168 *P. knowlesi* infections. The majority (n = 1,356) were generated from macaque-host *P.*
169 *knowlesi* infections, and all of these were generated by a single contributor from a small set of
170 laboratory-maintained Rhesus macaques (PRJNA508940, PRJNA526495, and
171 PRJNA524357). Sixty-one libraries were derived from cell culture, and the source of 52
172 (BioProject PRJEB24220) could not be determined. Thus, an accurate prevalence estimate of
173 the *P. knowlesi*-associated ormycovirus could not be obtained from this data set.

174

175 We next investigated the prevalence of ormycoviruses more broadly in disease-causing
176 Apicomplexa by screening 2,898 RNA SRA libraries (*Cryptosporidium*, *Coccidia*, *Toxoplasma*,
177 *Babesia*, and *Theileria*) (**Supp. Data 2**). This yielded identical ormyco-like RdRp segments in
178 the transcriptomes of 22 *Coccidia* (*Cystoisospora suis*) libraries, 21 of which belonged to the
179 same BioProject (PRJEB52768)⁶¹. The remaining library (SRR4213142) was published by the
180 same authors, suggesting that all 22 libraries were generated from the same source⁶². The
181 transcripts of the *Cystoisospora*-associated virus encoded complete ORFs with an NDD motif
182 C and were ~3.1kb in length (range: 3009-3203) (**Table S3**). This virus was highly divergent,
183 sharing only 32.5% identity (e-value = 6×10^{-37}) with its closest blast hit (Wildcat Canyon virus,
184 WZL61396.1). It was also at low abundance across the 22 libraries (range: 0.01-0.08% of non-
185 rRNA reads). We could not conclude that *C. suis* was the host because fungi represented
186 4.6% of the non-rRNA reads in a representative library (ERR9846867). Regardless, the
187 prevalence of ormycoviruses was 100% among *Cystoisospora suis* libraries but otherwise
188 very low in this data set (0.76%).

189

190 Phylogenetic analysis placed both Apicomplexa-associated viruses in the “Alpha” clade of the
191 ormycoviruses (**Fig. 1d**). The topology of the inferred phylogenies was stable across six
192 combinations of alignment and trimming methods and recapitulated the three main

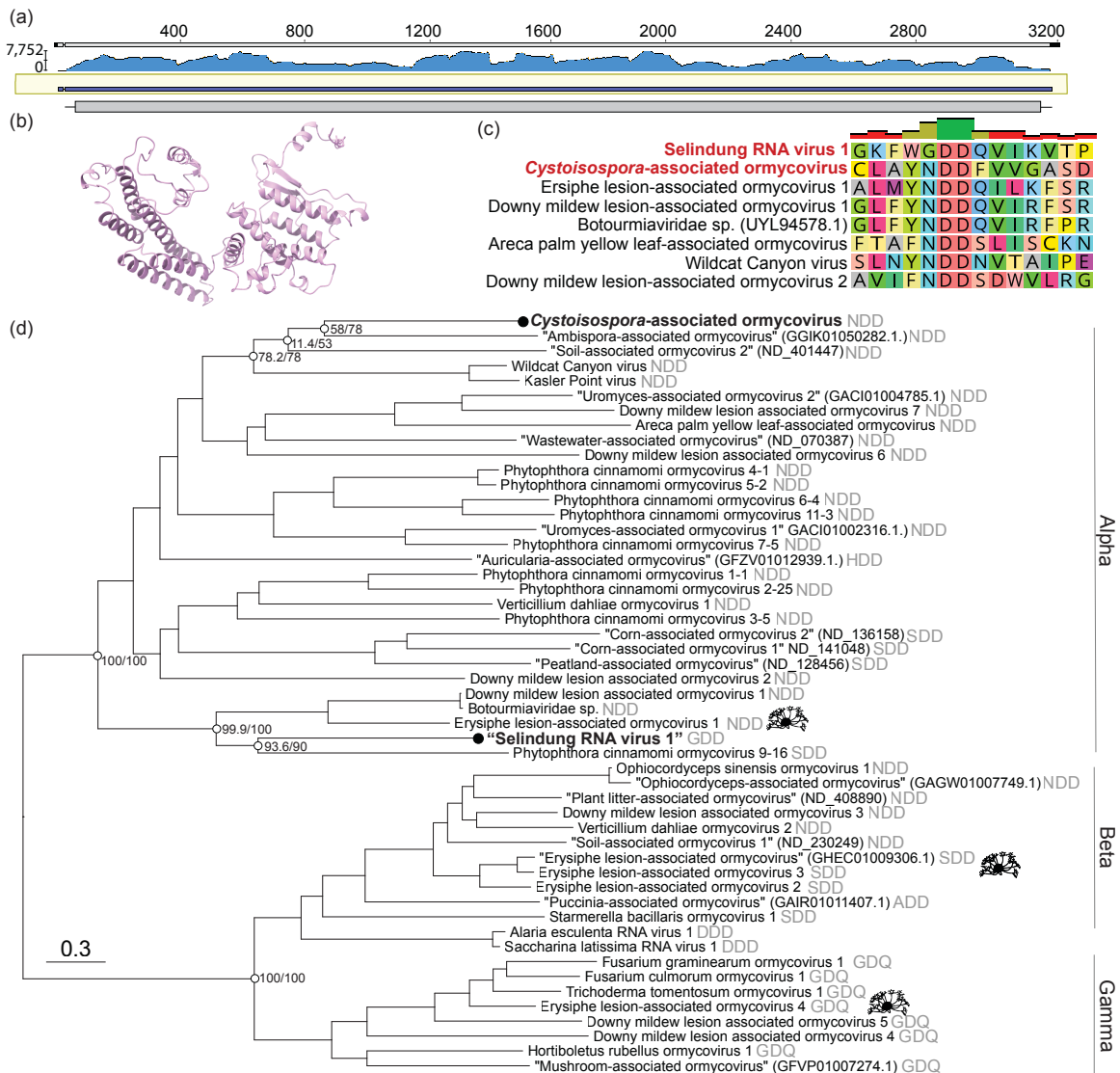
193 ormycovirus clades “Alpha”, “Beta”, and “Gamma”⁴⁷ with strong support (Fig. S2). Viruses did
 194 not cluster by host. For example, viruses associated with the fungal species *Erysiphe* fell
 195 across all three clades and encoded three different catalytic triads (Fig. 1d, icons), and the
 196 Apicomplexa-associated viruses were not closely related within the Alpha clade.

197

198 We concluded that the *P. knowlesi*-associated virus represents the first evidence of an RNA
 199 virus associated with *P. knowlesi* and constitutes only the second instance of an RNA virus
 200 associated with any *Plasmodium* species. We have provisionally named it “Selindung RNA
 201 virus 1” because it appeared to be concealed (“terselindung”, Bahasa Malaysia) within the
 202 *Plasmodium* parasite, and we will use this name herein.

203

204



205

206

207

208

209

Figure 1. A divergent RNA virus associated with human-infecting *P. knowlesi* is a member of the unclassified group ‘ormycovirus’. (a) Sequencing coverage of the RNA-dependent RNA polymerase (RdRp) of a *P. knowlesi*-associated viral contig. Trimmed reads were mapped to the assembled contig using BMap⁶³ and visualised with Geneious Prime

210 v2024.0.7. (b) The predicted structure of the putative hypothetical protein of Selindung RNA
211 virus 1. (c) MAFFT alignment of motif C in the palm domain of the *P. knowlesi*- and
212 *Cystoisospora*-associated viruses and representative ormycoviruses. (d) Phylogenetic
213 inference of the ormycoviruses aligned with MAFFT. The positions of *Erysiphe*-associated
214 viruses are denoted with black icons (source: phylopic.org). Black tip dots indicate viruses
215 identified in this study. Tips with names in quotes were previously identified but not named⁴⁷.
216 Their corresponding NCBI or RVMT accession is shown in parentheses. The catalytic triad
217 encoded in each palm domain is denoted in grey. Support values are shown at select nodes
218 as sh-aLRT/UFBboot. Tree branches are scaled to amino acid substitutions.

219
220

221 **Ormycoviruses are associated with arthropod metatranscriptomes**

222 In addition to expanding the diversity of *Plasmodium*-associated RNA viruses, Selindung RNA
223 virus 1 was of particular interest because it had evidently been transmitted along with its
224 *Plasmodium* host to a human via a mosquito vector. Taking this together with the detectable
225 phylogenetic relationship of this virus and two viruses recovered from tick metagenomes
226 (Wildcat Canyon virus and Kasler Point virus), we posited that ormycoviruses might exhibit a
227 complex ecology at the arthropod-mammal interface. We therefore sought to further extend
228 the known host range of ormycoviruses to the transcriptomes of the arthropods that indirectly
229 transmit them.

230

231 We screened the 4,864 arthropod libraries available on NCBI Transcriptome Shotgun
232 Assemblies (TSA) as of August 2024, initially using Kasler Point virus (WZL61394) as input
233 and then following an iterative process (see *Methods*). In this way we identified 15 putative
234 viruses associated with three of the four extant subphyla of the Arthropoda: Chelicerata (n =
235 1), Crustacea (n = 1), and Hexapoda (n = 13) (**Table S4**). All shared detectable but minimal
236 sequence similarity with published ormycoviruses (range: 27.1-41.0%, **Table S4**). Two
237 encoded GDD at motif C like Selindung RNA virus 1, while the remainder had NDD at this
238 position.

239

240 Phylogenetic analysis again supported the conclusion that these viruses are part of the
241 ormycovirus group (**Fig. 2a**). All viruses identified in this study fell in the Alpha clade. Selindung
242 RNA virus 1 formed a group with the other two GDD-encoding viruses (Beetle-associated
243 ormycovirus 1 and Bristletail-associated ormycovirus 1). This placement was consistent
244 across all six iterations of phylogenetic inference (**Fig. S3**). However, aside from this instance
245 and the Gamma clade (GDQ), minimal clustering of motifs was observed. In addition, although
246 the host organisms had been collected from all six inhabited continents, there was no
247 clustering of viruses by geographic region of sampling (**Fig. 2a**).

248

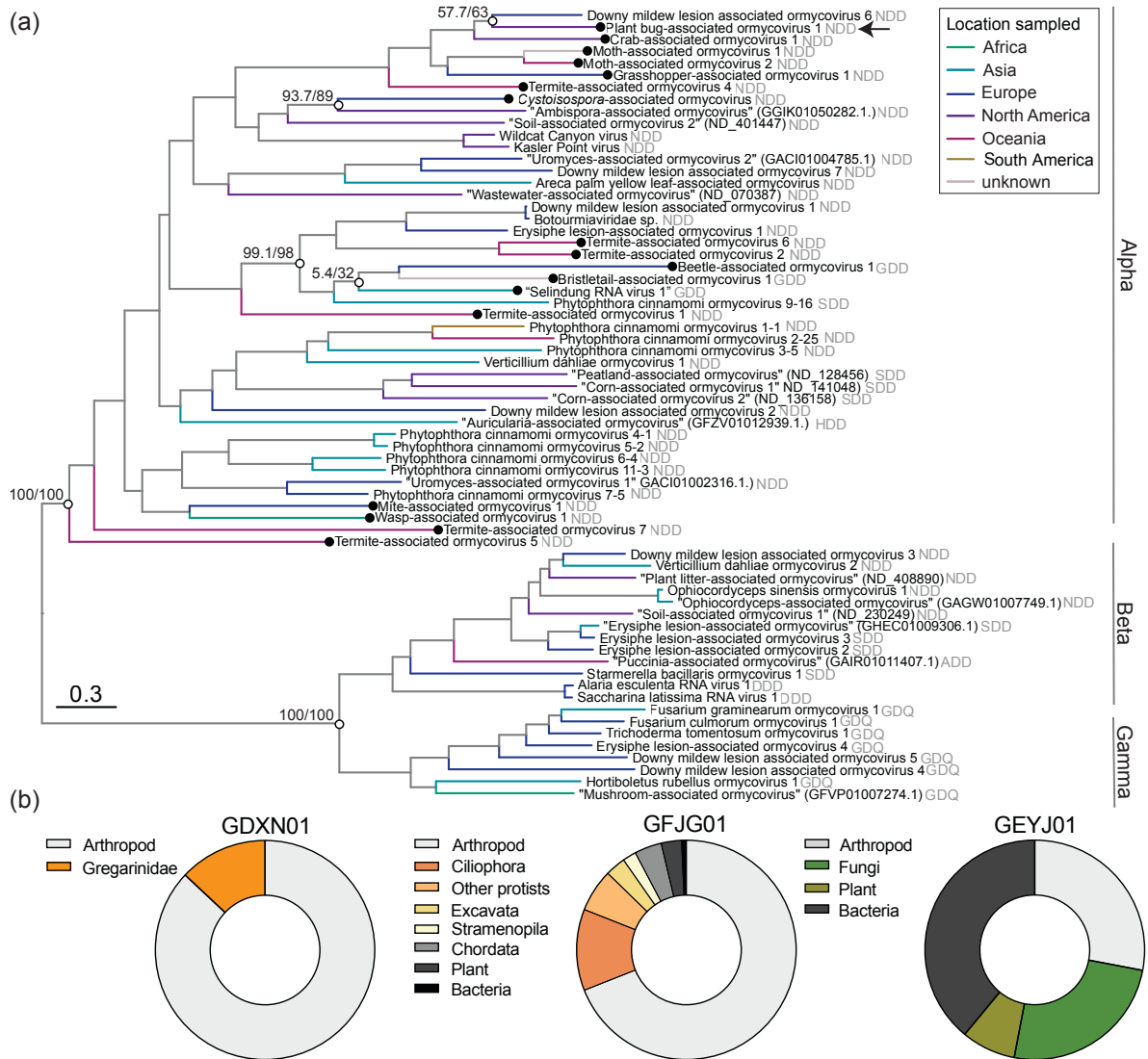
249 We concluded that at least some of these viruses were likely infecting single-celled organisms
250 rather than the arthropods themselves for two reasons. First, assessment of each library
251 composition revealed instances of parasitic hosts. Contigs mapping to alveolates accounted
252 for more than one tenth of one Hexapoda (GDXN01) and the only crustacean (GFJG01) library
253 (13% *Gregarinidae* and 12% Ciliophora, respectively) (**Fig 2b**). Similarly, the mite assembly
254 (GEYJ01) included 25% of contigs mapping to fungi (**Fig. 2b**). Second, the virus identified in
255 GBHO01 (*Lygus hesperus*) likely utilised the ciliate genetic code (i.e., only a truncated ORF
256 could be recovered with the standard genetic code) yet fell within the diversity of the taxon
257 (**Fig. 2a, Fig. S3, arrow**). Identical amino acid translations of the crustacean-associated virus
258 were produced when either the standard or the ciliate genetic code were used.

259

260 As with the *P. knowlesi* library, we searched these assemblies for hypothetical proteins. From
261 this, we identified a putative second segment in the *Machilis pallida* (Hexapoda) assembly
262 HBDP01 containing Bristletail-associated ormycovirus 1 that was 1,619bp in length and
263 encoded a partial ORF (HBDP01002991.1). We could not recover candidates corresponding
264 to the remaining libraries or assemblies.

265

266



267
 268 **Figure 2. Ormycoviruses are associated with arthropod transcriptomes.** (a) Phylogenetic
 269 inference of the extended diversity of ormycoviruses. Viruses identified in this study are
 270 indicated by black circles. The arrow indicates the position of the virus that appears to use the
 271 ciliate genetic code. Clades are annotated according to designations established by Forgia *et al.*⁴⁷.
 272 The catalytic triad encoded in each palm domain is denoted in grey. The tip labelling
 273 scheme for unnamed viruses (denoted by quotation marks) is the same as in Fig. 1. Support
 274 values are shown at select nodes as sh-aLRT/UFBoot. Tree branches are coloured by the
 275 location where each tip was sampled, and they are scaled by amino acid substitutions. (b)
 276 Library composition of select arthropod assemblies. The graph labels correspond to the TSA
 277 project ID.

278
 279

280 The ormycoviruses are members of a diverse and unclassified viral taxon

281 The wide host range of the ormycoviruses, spanning Alveolata, Stramenopila, and
 282 Opisthokonta (Fungi), suggested that this unclassified group harboured unrealised viral
 283 diversity. We therefore aimed to contextualise the diversity of the ormycoviruses within
 284 unclassified taxa identified in virus discovery studies. To do this, we assembled a custom
 285 database of the viruses identified using an artificial intelligence-based method⁵³ and screened

286 the ormycoviruses against it using DIAMOND Blastx⁶⁴. This approach placed ormycoviruses
287 within an unclassified taxon referred to in the original study as the proposed “SuperGroup
288 024”⁵³, a name which we will use herein.

289

290 Phylogenetic analysis illustrated that the current set of ormycoviruses represent only a fraction
291 of the total diversity of this group as they fell throughout the phylogeny. Interestingly, the
292 addition of the SuperGroup 024 viruses expanded the diversity of the Alpha group, scattering
293 the original members across three sections of the tree (**Fig. 3a, blue branches**). The Beta
294 and Gamma clades were unchanged and characterised by a long branch at their shared base
295 (**Fig. 3a, green and yellow branches**).

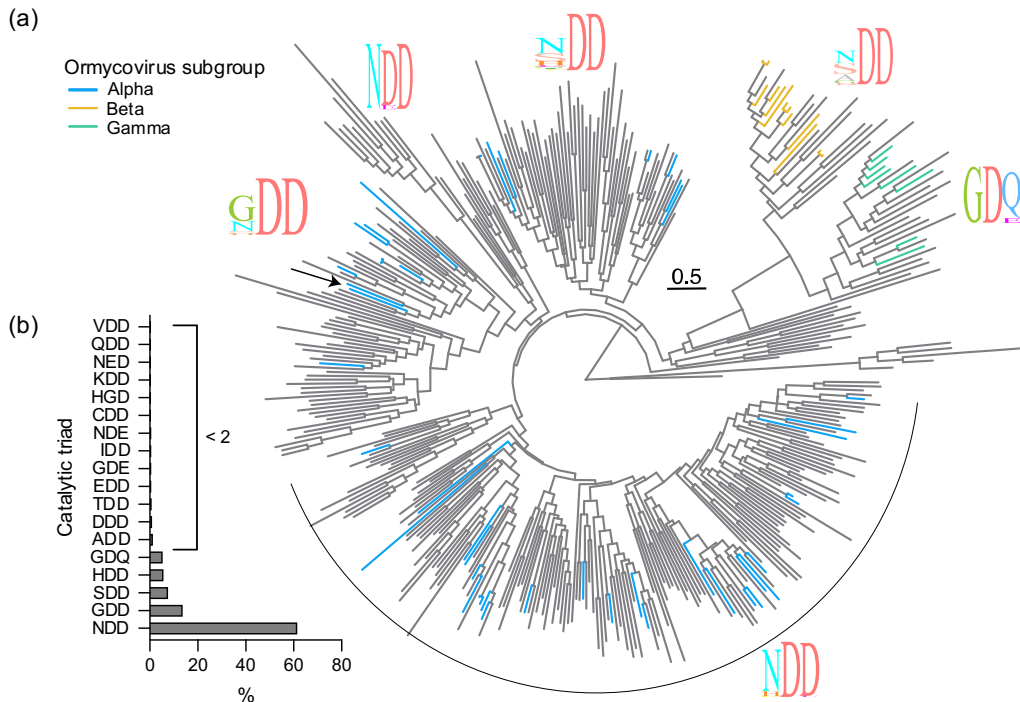
296

297 Members of SuperGroup 024 encoded a more diverse set of catalytic triads at the motif C
298 palm domain compared to the original ormycovirus data set⁴⁷ (**Fig 3b**). However, their addition
299 did not lead to observable clustering of discrete motif sequences, as flexibility was observed
300 throughout the phylogeny. Selindung RNA virus 1 again fell in a section predominated by GDD
301 at that position (**Fig. 3a, arrow**).

302

303 We searched the libraries containing SuperGroup 024 RdRp segments for ormycovirus
304 hypothetical proteins. Of the 259 SRA libraries in which SuperGroup 024 RdRps were detected
305 and assembled, we recovered hypothetical protein candidates at least 1000bp in length in 190
306 (73.4%). It was not possible to assign hypothetical proteins to corresponding RdRps as many
307 libraries contained multiple RdRp segments. Despite this, our finding supports the conclusion
308 that bisegmentation is a characteristic of viruses in this taxon and that ormycoviruses and
309 SuperGroup 024 are one and the same.

310



311
 312 **Figure 3. Ormycoviruses are members of a diverse and unclassified viral taxon with a**
 313 **flexible motif C in its palm domain.** (a) Phylogenetic inference of viruses in SuperGroup
 314 024⁵³. Branches are coloured by their placement in the ormycovirus-only phylogenetic tree
 315 (Fig. 1 and 2). Grey tree branches indicate that those tips were not previously recognised as
 316 ormycoviruses. The icons show the proportion of individual amino acids at each position of
 317 the catalytic triad in motif C of the RdRp palm domain for the corresponding clades. The arrow
 318 indicates the topological position of Selindung RNA virus 1. Tree branches are scaled
 319 according to amino acid substitutions. (b) Distribution of catalytic triads encoded by members
 320 of SuperGroup 024. The x-axis shows the percentage that each triad comprises among all
 321 known SuperGroup 024 species.

322

323

324 DISCUSSION

325 This study expands the diversity of *Plasmodium*-associated RNA viruses and presents the first
 326 evidence of an RNA virus associated with zoonotic transmission of *P. knowlesi*. Previously,
 327 only Matryoshka RNA virus 1 (*Narnaviridae*) had been identified in a *Plasmodium* species (the
 328 human-only *Plasmodium* species, *P. vivax*)^{40,41}. Although it is not possible to conclusively
 329 establish that Selindung RNA virus 1 was infecting the parasite from metatranscriptomic data
 330 alone, lines of indirect evidence suggest that it was. Most notably, no other probable hosts,
 331 including fungi, were identified in the library, and the RdRp contig was relatively abundant
 332 (1.4% of non-rRNA reads). Contamination was an unlikely source because neither the putative
 333 RdRp nor the second segment were detected in the other three libraries extracted and
 334 sequenced at the same time. In addition, we were able to confirm the presence of the RdRp
 335 segment in two of the six *P. knowlesi* isolates using PCR. We therefore concluded that
 336 Selindung RNA virus 1 most likely represents an RNA virus in a second *Plasmodium* species.

337 Robust sampling of natural *P. knowlesi* infections is needed to evaluate the prevalence and
338 pathobiology of Selindung RNA virus 1. We observed one instance of Selindung RNA virus 1
339 among 1,470 SRA libraries, which suggests that associations occur infrequently and contrasts
340 with the identification of Matryoshka RNA virus 1 in 13 of 30 *P. vivax* SRA libraries⁴⁰. However,
341 ours was the only library to have been generated from isolates collected from naturally infected
342 humans, while most of the publicly available data were derived from laboratory experiments.
343 The detection of the RdRp segment in two of six isolates in our library could indicate that
344 associations are more frequent in natural infections in Sabah, but our study was not powered
345 to assess this. Similarly, whether the observation that presence of the virus was correlated
346 with higher parasitemia is meaningful requires further epidemiological investigation.

347

348 Arthropods are a powerful tool for measuring the prevalence of viruses in nature, particularly
349 when sampling from humans or other vertebrates is not feasible. The identification of
350 ormycoviruses in arthropod metatranscriptomes and in a human blood sample suggests that
351 these viruses represent a unique type of arbovirus that can be transmitted as a passenger
352 between arthropods and mammals. Mosquito-based surveillance methods have been
353 proposed for tracking the incidence and spread of human pathogens^{65,66}. Unlike cell culture or
354 primary samples, which rely on symptomatic individuals with access to diagnostic testing,
355 arthropod-based surveillance would be relatively unbiased, enabling more accurate estimates
356 of protozoan virus prevalence and diversity within communities. When combined with cell
357 culture data, this approach could also be used to parse arthropod- and protozoan-infecting
358 viruses. Because they can be indirectly transmitted by arthropods, it may be that other
359 protozoan viruses have already been identified, but their relationship to their protozoan host
360 was obscured because they were part of an arthropod metatranscriptome.

361

362 An incidental and surprising finding was the identification of an ormycovirus that appears to
363 use a non-standard genetic code (Plant bug-associated ormycovirus 1). Despite this
364 difference, the virus fell within the diversity of the ormycoviruses and SuperGroup 024. As RNA
365 viruses are reliant on host machinery for translation, it was previously proposed that the
366 evolution of alternative genetic codes was an antiviral defence⁶⁷. Under this assumption, the
367 use of host-specific genetic codes by RNA viruses would imply a long-term virus-host
368 coevolutionary relationship, and we would not expect to find viral taxa in which members use
369 different genetic codes. Genetic code switching has been observed infrequently in the
370 *Picornavirales* and *Lenarviricota*⁶⁸. Whether these select instances are an aberration in an
371 otherwise broadly held rule of virology requires further investigation. However, we posit that
372 there may be many more instances of code switching within known viral taxa that have been
373 overlooked as a consequence of inadequate bioinformatic workflows. For example, if we had

374 used an automated pipeline that filtered out contigs that did not produce an ORF with the
375 standard genetic code, Plant bug-associated ormycovirus 1 would have been removed from
376 our data set. We therefore advocate for the inclusion of multiple genetic codes when searching
377 for divergent RNA viruses.

378

379 That Selindung RNA virus 1 does not belong to a known viral taxon is notable because it
380 demonstrates that parasitic protozoa likely harbour currently unrealised diversity, and
381 additional discoveries may be imminent as new bioinformatic tools are developed to explore
382 the RNA virosphere. However, the discovery of the ormycoviruses highlights the importance
383 of linking large-scale metatranscriptomic data to smaller-scale experimental work when
384 searching for protozoan viruses. Large-scale virus discovery studies often prioritise
385 environmental samples such as water⁵⁴, sediment⁵³, and soil⁶⁸ because these biodiverse
386 sources are rich with RNA viruses. Yet, this approach cannot distinguish between bacterial-,
387 archaeal-, and eukaryotic-infecting RNA viruses. Without the discovery of the ormycoviruses
388 and the experimental validation by Forgia *et al.*⁴⁷, SuperGroup 024 would have been
389 overlooked as a potential source of protozoan virus candidates. Similarly, large-scale studies
390 are not equipped to distinguish segmented from non-segmented viruses because they
391 necessarily focus on detecting RdRps, rendering them “blind” to segmentation. The molecular
392 characterisation of the ormycoviruses again demonstrates this limitation because their
393 hypothetical protein does not share detectable sequence or structural similarity with known
394 viral proteins. Without the incidental finding by Forgia *et al.*⁴⁷, we would not have been able to
395 infer that the ormycoviruses and the members of SuperGroup 024 are likely segmented
396 viruses.

397

398 This, as with other metagenomic studies, primarily serves to generate hypotheses and raise
399 questions about RNA virus evolution and biology that require additional experimental data to
400 answer. It is not known whether the ormycoviruses are positive- or negative-sense viruses.
401 Forgia *et al.* proposed that they are negative-sense because they observed a higher proportion
402 of negative-sense RNA in their samples⁴⁷; however, this is not definitive. The presence of both
403 SDD and GDD catalytic triads in motif C in the palm domain counters the hypothesis that SDD
404 is specific to segmented negative-sense RNA viruses⁶⁹, although it is possible that
405 ormycoviruses do indeed fall into this category. The flexibility of the catalytic triad also raises
406 the question of whether individual triads have a detectable impact on the biology of the virus
407 and why flexibility is permitted in otherwise highly conserved region of the virus genome. From
408 a global health perspective, the most important questions to address include how viral infection
409 of *Plasmodium* affects onward *Plasmodium* transmission and the pathobiology of *Plasmodium*
410 in humans. Additionally, which part of the parasite the virus infects and whether this could be

411 used as a potential drug target remain unanswered. It has already been shown that viruses
412 can serve as a weapon against drug-resistant bacterial infections²³⁻²⁵. Whether a similar
413 approach could be deployed to combat malaria and other disease-causing Apicomplexa
414 should be a research priority.

415

416 **METHODS**

417 **Human malaria isolates**

418 *Plasmodium* RNA was isolated from cryopreserved red cells collected from 18 patients with
419 acute malaria, enrolled in Kudat Division, Sabah, Malaysia in 2013 and 2014¹⁵. PCR was used
420 to confirm *Plasmodium* species as *P. knowlesi* (n=6), *P. vivax* (n=7) and *P. falciparum* (n=5),
421 as previously reported⁴⁰.

422

423 **SRA library data sets**

424 *BioProject PRJNA589654 libraries*

425 *Plasmodium* SRA libraries in BioProject PRJNA589654 (n = 4) (i.e., the BioProject that
426 contained Matryoshka RNA virus 1) were downloaded from NCBI. Nextera adapters were
427 trimmed using Cutadapt v.1.8.3⁷⁰ with the parameters removing 5 bases from the beginning
428 and end of each read, a quality cutoff of 24, and a minimum length threshold of 25. The quality
429 of trimming was assessed using FastQC v0.11.8⁷¹. rRNA reads were removed using
430 SortMeRNA v4.3.3⁷², and non-rRNA reads were assembled using MEGAHIT v1.2.9⁷³.

431

432 *Disease-causing Apicomplexa libraries*

433 We downloaded all *P. knowlesi* RNA SRA libraries of at least 0.5Gb in size available on NCBI
434 as of August 2024 (n = 1,470). We also downloaded all RNA SRA libraries for *Cryptosporidium*,
435 *Coccidia*, *Toxoplasmosis*, *Babesia*, and *Theileria* available on NCBI as of March 2024 that are
436 at least 0.5Gb in size and generated on the Illumina platform (n = 3,162).

437

438 *SuperGroup 024 libraries*

439 To analyse the libraries containing RdRp segments of so-called SuperGroup 024⁵³, we first
440 downloaded all of the contigs designated in this group by Hou *et al.*⁵³ (<http://47.93.21.181/>).
441 We then extracted the corresponding SRA libraries from each sequence header and removed
442 duplicates (n = 273). All but one were downloaded from NCBI. The library SRR1027962 failed
443 repeated attempts to download, likely due to its size (99.8Gb).

444

445 **Arthropod Transcriptome Shotgun Assemblies (TSA) screen**

446 We began by screening all arthropod TSA (n = 4,864) available in August 2024, using Kasler
447 Point virus (a tick-associated ormycovirus) as input. This screen was performed with tBLASTn

448 implemented in the NCBI Blast web interface (<https://blast.ncbi.nlm.nih.gov/Blast.cgi>). All hits
449 were reviewed and filtered according to three criteria: (1) the contig was at least 800bp in
450 length, (2) the contig encoded an uninterrupted ORF, (3) the contig did not return any hits to
451 cellular genes when screened against the NCBI non-redundant (nr) database. We then aligned
452 our filtered data set using MAFFT⁷⁴ with default parameters, and selected the most divergent
453 virus according to the distance matrix. This virus was then used as input for an additional
454 screen of the arthropod TSA. This process was repeated until no new contigs were identified.

455

456 **Library processing**

457 *Contig assembly*

458 For all data sets obtained from the SRA, Nextera adapters were trimmed using Cutadapt
459 v.1.8.3⁷⁰ with the parameters described above. The efficacy of trimming was assessed using
460 FastQC v0.11.8⁷¹. In total, 1,470 *P. knowlesi* libraries, 2,898 additional Apicomplexa libraries,
461 and 259 libraries included by Hou *et al.*,⁵³ were successfully assembled using MEGAHIT
462 v1.2.9⁷³.

463

464 *Abundance estimates*

465 The expected count of putative viral transcripts was inferred using RSEM v1.3.0⁷⁵. For the *P.*
466 *knowlesi* library containing the ormycovirus (SRR10448860), reverse-strandedness was
467 specified to match the sequencing protocol. Default parameters were used for the remaining
468 libraries. To infer the proportion of reads of each putative viral transcript, we calculated the
469 total expected count for the isoforms in each library and used this value as the denominator
470 to measure the percentage that putative viral reads comprised in the library. This analysis was
471 performed in R v4.4.0.

472

473 **Identification of divergent viruses**

474 *Polymerase segment identification*

475 We identified Selindung RNA virus 1 using the RdRp-scan workflow⁵⁵. Briefly, we screened
476 the protein sequence and HMM-profile of assembled contigs from each library against a viral
477 RdRp database. To search for additional divergent viruses, we screened all SRA libraries
478 against the RdRp-scan database⁵⁵ and a custom database containing known ormycoviruses
479 using DIAMOND Blastx v2.0.9⁶⁴ and the setting 'ultra-sensitive'. This database included the
480 39 published ormycoviruses and the Selindung RNA virus 1 RdRp segment. Only hits with e-
481 values below 1e-07 were retained for further analysis. Contigs with hits to this database were
482 then screened against the NCBI nr protein database to remove false positives, again using
483 DIAMOND Blastx v2.0.9⁶⁴ and an e-value threshold of 1e-07. The parameter 'very-sensitive'
484 was specified. Contigs that shared detectable sequence similarity to cellular genes were

485 excluded from further analysis. Nucleotide sequences were translated using Expasy
486 (<https://web.expasy.org/translate/>). The standard genetic code was used by default. Contigs
487 that did not return an ORF in any frame with this code were checked manually using all codes
488 available in Expasy.

489

490 *Second segment identification*

491 We first used blastn to screen libraries for contigs sharing conserved 5' and 3' termini of the
492 corresponding ormycovirus RdRp. When this did not reveal any candidates, we compiled a
493 database of all known ormycovirus second segments and used this to screen all SRA libraries
494 using DIAMOND Blastx v2.0.9⁶⁴. Contigs that had statistically significant hits to this database
495 were checked against the NCBI nr protein database to remove false positives (i.e., cellular
496 genes). Nucleotide sequences were either translated individually with Expasy
497 (<https://web.expasy.org/translate/>) or with InterProScan v5.65-97.0. For sequences processed
498 with the latter, the longest translated ORFs were used for downstream analysis. To tally the
499 number of SuperGroup 024 libraries with detectable hypothetical proteins, we cross-checked
500 the presence of RdRp segments and hypothetical protein segments in each library using R
501 v4.4.0.

502

503 For the primary *P. knowlesi* library, we searched for similar sequences to those at the 5' and
504 3' termini of the RdRp segment in other contigs in the library. To do this, we extracted these
505 regions from the RdRp segment and used each as input for tblastn against the assembled
506 library (SRR10448860). To ensure that the putative Selindung RNA virus 1 hypothetical protein
507 was not present in other libraries in the same BioProject, we used this sequence as input for
508 tblastn against the three remaining libraries.

509

510 Both tblastn screens were implemented in Geneious Prime v2024.0.7 and default parameters
511 were used.

512

513 *PCR validation*

514 We first generated cDNA from the isolates using the SuperScript IV reverse transcriptase
515 (Invitrogen). These products were then used as templates for amplification with PCR.
516 Reactions were carried out in a total volume of 50ul, of which 25ul was SuperFi II (Invitrogen)
517 master mix and 1ul was the cDNA template. 2.5ul of forward and reverse primers were used
518 (**Table S1**). Reactions were performed on a thermocycler with the following conditions: 98°C
519 for 1 min followed by 35 cycles of 98°C for 10s, 60°C for 10s, 72°C for 1 min, and 72°C for 5
520 min. The PCR products were analysed on an agarose gel. We used *Plasmodium* LDHP
521 primers as the positive control.

522

523 **Library composition analysis**

524 *CCMetagen*

525 The composition of individual sequencing libraries was assessed using ccmetsagen v1.2.4⁵⁹
526 and kma v1.3.9a⁶⁰ using assembled contigs as input. The results presented in **Fig. 2b** were
527 visualised with Prism v.10.3.0.

528

529 **Protein structure inference**

530 The structure of the putative hypothetical proteins of Selindung RNA virus 1 and Erysiphe
531 lesion-associated ormycovirus 1 were predicted using AlphaFold2^{56,57} implemented in the
532 Google Colab cloud computing platform. The confidence (as measured by pLDDT) of the
533 prediction was compared across five models, and the highest performing models (Selindung
534 RNA virus 1: #2, Erysiphe lesion-associated ormycovirus 1: #4) were selected for downstream
535 analysis (**Fig. S4**). To assess structural similarity, we performed a pairwise alignment of the
536 resulting pdb files of each predicted structure using FatCat⁵⁸. All pdb files were visualised in
537 ChimeraX v1.7.1⁷⁶.

538

539 **Functional domain inference**

540 Several approaches were used to infer functional domains in the hypothetical protein, although
541 none were successful. We first performed a preliminary check with InterProScan⁷⁷, screening
542 against the CDD, NCBIfam, and TMHMM databases. This approach was implemented in
543 Geneious Prime v2024.0.7. We then employed Phyre2⁷⁸ and HHPred⁷⁹ using PDB. Finally, we
544 used the predicted structure of the hypothetical protein of Selindung RNA virus 1 as input for
545 FoldSeek⁸⁰, implemented on the Foldseek Server.

546

547 **Phylogenetic analysis**

548 To assess the phylogenetic relationships of the ormycoviruses identified in this study with
549 those documented previously, we compiled a data set of all known ormycoviruses. This
550 comprised 36 ormycoviruses⁴⁷⁻⁵² and unclassified or misclassified ormycoviruses that shared
551 detectable sequence similarity with known ormycoviruses: Wildcat Canyon virus (WZL61396),
552 Kasler Point virus (WZL61394), and a fungus-associated “Botourmiaviridae” (UYL94578). For
553 the SuperGroup 024 analysis, we utilised the data set featured in the phylogenetic analysis
554 presented by Hou *et al.*⁵³.

555

556 We first added the *P. knowlesi*- and *Cystoisospora*-associated viruses identified in this study
557 to the ormycovirus data set and aligned with MAFFT v7.490⁸¹ and MUSCLE v5.1⁸².
558 Ambiguities in each alignment were considered in three ways using trimAl v1.4.1⁸³: (i) no

559 ambiguities were removed; (ii) ambiguities were removed using a gap threshold of 0.5 and a
560 conservation percentage of 50; (iii) ambiguities were removed using the parameter
561 “gappyout”. Phylogenetic trees for these six alignments were inferred using ModelFinder and
562 IQ-TREE v1.6.12⁸⁴. To quantify support for the topology, we again used 1000 ultra-fast
563 bootstraps and 1000 SH-aLRT bootstrap replicates.

564

565 To infer the pan-SuperGroup 024 phylogeny, all amino acid sequences were aligned using
566 both MAFFT v7.490⁸¹ and MUSCLE v5.1⁸². Ambiguities were removed using trimAl v1.4.1⁸³
567 and the parameter -gappyout. The phylogenetic tree was inferred using IQ-TREE v1.6.12⁸⁴
568 with ModelFinder limited to LG. Support values were measured with 1000 ultra-fast bootstraps
569 (UFboot) and 1000 sh-aLRT bootstrap replicates.

570

571 All trees were visualised with ggtree^{85,86} (implemented in R v4.4.0) and Adobe Illustrator
572 v26.4.1.

573

574 **Motif C tally and visualisation**

575 The catalytic triad encoded by each virus in SuperGroup 024 was recorded and tabulated
576 using R v4.4.0. The results were visualised with Prism v.10.3.0.

577

578 Sequences from individual clades were extracted from the SuperGroup 024 phylogeny by
579 selecting individual nodes using the function “extract.clade()” implemented in the R package
580 ape. Sequences from each clade were then realigned with MAFFT and the motif C logos were
581 generated according to the consensus sequence in Geneious Prime v2024.0.7.

582

583 **DATA AVAILABILITY**

584 All sequencing data analysed in this study are publicly available on NCBI (ormycoviruses) and
585 an independent repository (<http://47.93.21.181/>, SuperGroup 024). Assembled contigs for the
586 viruses identified in this study, the custom database used to screen libraries, alignments, and
587 tree files are available on GitHub (https://github.com/mary-petrone/Plasmodium_ormyco).

588

589 **ACKNOWLEDGMENTS**

590 This work was funded by a National Health and Medical Research Council (NHMRC)
591 Investigator award (MJG), AIR@InnoHK administered by the Innovation and Technology
592 Commission, Hong Kong Special Administrative Region, China (ECH), a Sydney ID Seed
593 Funding Award (MEP), and the National Institutes of Health, USA R01 AI160457-01 and
594 Malaysia Ministry of Health Grant BP00500/117/1002 (GSR). We thank the Director General
595 of Health, Malaysia for the permission to publish this article.

596 We also thank Jon Mifsud for his BatchArtemisSRAMiner pipeline
597 (<https://github.com/JonathonMifsud/BatchArtemisSRAMiner>), which we used for all SRA
598 screens, and Dr. Alvin Kuo Jing Teo for suggesting the name Selindung RNA virus 1.

599

600 **AUTHOR CONTRIBUTIONS**

601 M.E.P., J.C., N.M.A., and E.C.H. designed the study. M.J.G, T.W., G.R., J.W., and K.A.P.
602 designed the original malaria studies and collected the samples. M.E.P., J.C., and M.S.
603 performed the experiments and analyses. M.E.P. wrote the initial manuscript draft. All authors
604 reviewed and edited the manuscript.

605
606
607
608
609
610
611
612
613
614
615
616
617
618
619
620
621
622
623
624
625
626
627
628
629
630
631
632
633
634
635
636
637
638
639
640
641
642
643
644
645
646
647
648
649
650
651
652
653
654
655
656
657
658

REFERENCES

- 1 Aguirre, A. A. *et al.* The One Health Approach to Toxoplasmosis: Epidemiology, Control, and Prevention Strategies. *Ecohealth* **16**, 378-390 (2019). <https://doi.org/10.1007/s10393-019-01405-7>
- 2 Ryan, U., Fayer, R. & Xiao, L. Cryptosporidium species in humans and animals: current understanding and research needs. *Parasitology* **141**, 1667-1685 (2014). <https://doi.org/10.1017/s0031182014001085>
- 3 Krause, P. J. Human babesiosis. *Int J Parasitol* **49**, 165-174 (2019). <https://doi.org/10.1016/j.ijpara.2018.11.007>
- 4 Poespoprodjo, J. R., Douglas, N. M., Ansong, D., Kho, S. & Anstey, N. M. Malaria. *Lancet* **402**, 2328-2345 (2023). [https://doi.org/10.1016/S0140-6736\(23\)01249-7](https://doi.org/10.1016/S0140-6736(23)01249-7)
- 5 Malaria, <<https://www.who.int/news-room/fact-sheets/detail/malaria>> (2023).
- 6 Lee, W. C. *et al.* Plasmodium knowlesi: the game changer for malaria eradication. *Malar J* **21**, 140 (2022). <https://doi.org/10.1186/s12936-022-04131-8>
- 7 Wellems, T. E. & Plowe, C. V. Chloroquine-Resistant Malaria. *The Journal of Infectious Diseases* **184**, 770-776 (2001). <https://doi.org/10.1086/322858>
- 8 Rosenthal, P. J. *et al.* The emergence of artemisinin partial resistance in Africa: how do we respond? *Lancet Infect Dis* (2024). [https://doi.org/10.1016/s1473-3099\(24\)00141-5](https://doi.org/10.1016/s1473-3099(24)00141-5)
- 9 Blasco, B., Leroy, D. & Fidock, D. A. Antimalarial drug resistance: linking Plasmodium falciparum parasite biology to the clinic. *Nat Med* **23**, 917-928 (2017). <https://doi.org/10.1038/nm.4381>
- 10 Ehrlich, H. Y., Jones, J. & Parikh, S. Molecular surveillance of antimalarial partner drug resistance in sub-Saharan Africa: a spatial-temporal evidence mapping study. *Lancet Microbe* **1**, e209-e217 (2020). [https://doi.org/10.1016/s2666-5247\(20\)30094-x](https://doi.org/10.1016/s2666-5247(20)30094-x)
- 11 Conrad, M. D. *et al.* Evolution of Partial Resistance to Artemisinins in Malaria Parasites in Uganda. *N Engl J Med* **389**, 722-732 (2023). <https://doi.org/10.1056/NEJMoa2211803>
- 12 Fornace, K. M. *et al.* No evidence of sustained nonzoonotic Plasmodium knowlesi transmission in Malaysia from modelling malaria case data. *Nature Communications* **14**, 2945 (2023). <https://doi.org/10.1038/s41467-023-38476-8>
- 13 Anstey, N. M. *et al.* Knowlesi malaria: Human risk factors, clinical spectrum, and pathophysiology. *Adv Parasitol* **113**, 1-43 (2021). <https://doi.org/10.1016/bs.apar.2021.08.001>
- 14 Rajahram, G. S. *et al.* Deaths From Plasmodium knowlesi Malaria: Case Series and Systematic Review. *Clin Infect Dis* **69**, 1703-1711 (2019). <https://doi.org/10.1093/cid/ciz011>
- 15 Grigg, M. J. *et al.* Age-Related Clinical Spectrum of Plasmodium knowlesi Malaria and Predictors of Severity. *Clin Infect Dis* **67**, 350-359 (2018). <https://doi.org/10.1093/cid/ciy065>
- 16 Cox-Singh, J. *et al.* Plasmodium knowlesi Malaria in Humans Is Widely Distributed and Potentially Life Threatening. *Clinical Infectious Diseases* **46**, 165-171 (2008). <https://doi.org/10.1086/524888>
- 17 Cooper, D. J. *et al.* Plasmodium knowlesi Malaria in Sabah, Malaysia, 2015-2017: Ongoing Increase in Incidence Despite Near-elimination of the Human-only Plasmodium Species. *Clin Infect Dis* **70**, 361-367 (2020). <https://doi.org/10.1093/cid/ciz237>
- 18 Tobin, R. J. *et al.* Updating estimates of Plasmodium knowlesi malaria risk in response to changing land use patterns across Southeast Asia. *PLoS Negl Trop Dis* **18**, e0011570 (2024). <https://doi.org/10.1371/journal.pntd.0011570>
- 19 Brock, P. M. *et al.* Predictive analysis across spatial scales links zoonotic malaria to deforestation. *Proc Biol Sci* **286**, 20182351 (2019). <https://doi.org/10.1098/rspb.2018.2351>

- 659 20 Fornace, K. M. *et al.* Environmental risk factors and exposure to the zoonotic malaria
660 parasite *Plasmodium knowlesi* across northern Sabah, Malaysia: a population-based
661 cross-sectional survey. *Lancet Planet Health* **3**, e179-e186 (2019).
662 [https://doi.org:10.1016/S2542-5196\(19\)30045-2](https://doi.org/10.1016/S2542-5196(19)30045-2)
- 663 21 Grigg, M. J. *et al.* Individual-level factors associated with the risk of acquiring human
664 *Plasmodium knowlesi* malaria in Malaysia: a case-control study. *Lancet Planet Health*
665 **1**, e97-e104 (2017). [https://doi.org:10.1016/S2542-5196\(17\)30031-1](https://doi.org/10.1016/S2542-5196(17)30031-1)
- 666 22 Anstey, N. M. & Grigg, M. J. Zoonotic Malaria: The Better You Look, the More You
667 Find. *J Infect Dis* **219**, 679-681 (2019). [https://doi.org:10.1093/infdis/jiy520](https://doi.org/10.1093/infdis/jiy520)
- 668 23 Hatfull, G. F., Dedrick, R. M. & Schooley, R. T. Phage Therapy for Antibiotic-Resistant
669 Bacterial Infections. *Annu Rev Med* **73**, 197-211 (2022).
670 [https://doi.org:10.1146/annurev-med-080219-122208](https://doi.org/10.1146/annurev-med-080219-122208)
- 671 24 Kortright, K. E., Chan, B. K., Koff, J. L. & Turner, P. E. Phage Therapy: A Renewed
672 Approach to Combat Antibiotic-Resistant Bacteria. *Cell Host Microbe* **25**, 219-232
673 (2019). [https://doi.org:10.1016/j.chom.2019.01.014](https://doi.org/10.1016/j.chom.2019.01.014)
- 674 25 Strathdee, S. A., Hatfull, G. F., Mutalik, V. K. & Schooley, R. T. Phage therapy: From
675 biological mechanisms to future directions. *Cell* **186**, 17-31 (2023).
676 [https://doi.org:10.1016/j.cell.2022.11.017](https://doi.org/10.1016/j.cell.2022.11.017)
- 677 26 Barrow, P. *et al.* Viruses of protozoan parasites and viral therapy: Is the time now
678 right? *Virology* **17**, 142 (2020). [https://doi.org:10.1186/s12985-020-01410-1](https://doi.org/10.1186/s12985-020-01410-1)
- 679 27 Zhao, Z. *et al.* Multiple Regulations of Parasitic Protozoan Viruses: A Double-Edged
680 Sword for Protozoa. *mBio* **14**, e0264222 (2023). [https://doi.org:10.1128/mbio.02642-
681 22](https://doi.org/10.1128/mbio.02642-22)
- 682 28 Adjou, K. T. *et al.* First identification of *Cryptosporidium parvum* virus 1 (CSpV1) in
683 various subtypes of *Cryptosporidium parvum* from diarrheic calves, lambs and goat
684 kids from France. *Vet Res* **54**, 66 (2023). [https://doi.org:10.1186/s13567-023-01196-4](https://doi.org/10.1186/s13567-023-01196-4)
- 685 29 Berber, E., Şimşek, E., Çanakoğlu, N., Sürsal, N. & Gençay Göksu, A. Newly
686 identified *Cryptosporidium parvum* virus-1 from newborn calf diarrhoea in Turkey.
687 *Transbound Emerg Dis* **68**, 2571-2580 (2021). [https://doi.org:10.1111/tbed.13929](https://doi.org/10.1111/tbed.13929)
- 688 30 Ellis, J. & Revets, H. *Eimeria* species which infect the chicken contain virus-like RNA
689 molecules. *Parasitology* **101 Pt 2**, 163-169 (1990).
690 [https://doi.org:10.1017/s0031182000063198](https://doi.org/10.1017/s0031182000063198)
- 691 31 Han, Q. *et al.* Virus-like particles in *Eimeria tenella* are associated with multiple RNA
692 segments. *Exp Parasitol* **127**, 646-650 (2011).
693 [https://doi.org:10.1016/j.exppara.2010.12.005](https://doi.org/10.1016/j.exppara.2010.12.005)
- 694 32 Lee, S. & Fernando, M. A. Viral double-stranded RNAs of *Eimeria* spp. of the
695 domestic fowl: analysis of genetic relatedness and divergence among various strains.
696 *Parasitol Res* **86**, 733-737 (2000). [https://doi.org:10.1007/pl00008560](https://doi.org/10.1007/pl00008560)
- 697 33 Lee, S. & Fernando, M. A. Intracellular localization of viral RNA in *Eimeria necatrix* of
698 the domestic fowl. *Parasitol Res* **84**, 601-606 (1998).
699 [https://doi.org:10.1007/s004360050458](https://doi.org/10.1007/s004360050458)
- 700 34 Lee, S., Fernando, M. A. & Nagy, E. dsRNA associated with virus-like particles in
701 *Eimeria* spp. of the domestic fowl. *Parasitol Res* **82**, 518-523 (1996).
702 [https://doi.org:10.1007/s004360050155](https://doi.org/10.1007/s004360050155)
- 703 35 Revets, H. *et al.* Identification of virus-like particles in *Eimeria stiedae*. *Mol Biochem*
704 *Parasitol* **36**, 209-215 (1989). [https://doi.org:10.1016/0166-6851\(89\)90168-0](https://doi.org/10.1016/0166-6851(89)90168-0)
- 705 36 Roditi, I., Wyler, T., Smith, N. & Braun, R. Virus-like particles in *Eimeria nieschulzi* are
706 associated with multiple RNA segments. *Mol Biochem Parasitol* **63**, 275-282 (1994).
707 [https://doi.org:10.1016/0166-6851\(94\)90063-9](https://doi.org/10.1016/0166-6851(94)90063-9)
- 708 37 Wu, B. *et al.* *Eimeria tenella*: a novel dsRNA virus in *E. tenella* and its complete
709 genome sequence analysis. *Virus Genes* **52**, 244-252 (2016).
710 [https://doi.org:10.1007/s11262-016-1295-0](https://doi.org/10.1007/s11262-016-1295-0)
- 711 38 Xin, C. *et al.* Complete genome sequence and evolution analysis of *Eimeria stiedae*
712 RNA virus 1, a novel member of the family Totiviridae. *Arch Virol* **161**, 3571-3576
713 (2016). [https://doi.org:10.1007/s00705-016-3020-7](https://doi.org/10.1007/s00705-016-3020-7)

- 714 39 Gupta, P. *et al.* A parasite odyssey: An RNA virus concealed in *Toxoplasma gondii*.
715 *Virus Evolution* **10** (2024). <https://doi.org/10.1093/ve/veae040>
- 716 40 Charon, J. *et al.* Novel RNA viruses associated with *Plasmodium vivax* in human
717 malaria and *Leucocytozoon* parasites in avian disease. *PLoS Pathog* **15**, e1008216
718 (2019). <https://doi.org/10.1371/journal.ppat.1008216>
- 719 41 Kim, A., Popovici, J., Menard, D. & Serre, D. *Plasmodium vivax* transcriptomes reveal
720 stage-specific chloroquine response and differential regulation of male and female
721 gametocytes. *Nat Commun* **10**, 371 (2019). <https://doi.org/10.1038/s41467-019-08312-z>
- 722 42 Hotzel, I. *et al.* Extrachromosomal nucleic acids in bovine *Babesia*. *Mem Inst*
723 *Oswaldo Cruz* **87 Suppl 3**, 101-102 (1992). <https://doi.org/10.1590/s0074-02761992000700014>
- 724 43 Johnston, R. C. *et al.* A putative RNA virus in *Babesia bovis*. *Molecular and*
725 *Biochemical Parasitology* **45**, 155-158 (1991).
726 [https://doi.org/10.1016/0166-6851\(91\)90037-7](https://doi.org/10.1016/0166-6851(91)90037-7)
- 727 44 Heeren, S. *et al.* Diversity and dissemination of viruses in pathogenic protozoa. *Nat*
728 *Commun* **14**, 8343 (2023). <https://doi.org/10.1038/s41467-023-44085-2>
- 729 45 Atayde, V. D. *et al.* Exploitation of the *Leishmania* exosomal pathway by *Leishmania*
730 RNA virus 1. *Nat Microbiol* **4**, 714-723 (2019). <https://doi.org/10.1038/s41564-018-0352-y>
- 731 46 Deng, S. *et al.* *Cryptosporidium* uses CSpV1 to activate host type I interferon and
732 attenuate antiparasitic defenses. *Nat Commun* **14**, 1456 (2023).
733 <https://doi.org/10.1038/s41467-023-37129-0>
- 734 47 Forgia, M. *et al.* Three new clades of putative viral RNA-dependent RNA
735 polymerases with rare or unique catalytic triads discovered in libraries of ORFans
736 from powdery mildews and the yeast of oenological interest *Starmerella bacillaris*.
737 *Virus Evolution* **8** (2022). <https://doi.org/10.1093/ve/veac038>
- 738 48 Dekker, R. J. *et al.* Discovery of novel RNA viruses in commercially relevant
739 seaweeds *Alaria esculenta* and *Saccharina latissima*. *bioRxiv*,
740 2024.2005.2022.594653 (2024). <https://doi.org/10.1101/2024.05.22.594653>
- 741 49 Martyn, C. *et al.* Metatranscriptomic investigation of single *Ixodes pacificus* ticks
742 reveals diverse microbes, viruses, and novel mRNA-like endogenous viral elements.
743 *mSystems* **9**, e00321-00324 (2024). <https://doi.org/10.1128/msystems.00321-24>
- 744 50 Niu, X. *et al.* A Putative Ormycovirus That Possibly Contributes to the Yellow Leaf
745 Disease of Areca Palm. *Forests* **15**, 1025 (2024).
- 746 51 Pagnoni, S. *et al.* A collection of *Trichoderma* isolates from natural environments
747 in Sardinia reveals a complex virome that includes negative-sense fungal viruses
748 with unprecedented genome organizations. *Virus Evolution* **9** (2023).
749 <https://doi.org/10.1093/ve/vead042>
- 750 52 Sahin, E., Edis, G., Keskin, E. & Akata, I. Molecular characterization of the complete
751 genome of a novel ormycovirus infecting the ectomycorrhizal fungus *Hortiboletus*
752 *rubellus*. *Arch Virol* **169**, 110 (2024). <https://doi.org/10.1007/s00705-024-06027-1>
- 753 53 Hou, X. *et al.* Artificial intelligence redefines RNA virus discovery. *bioRxiv*,
754 2023.2004.2018.537342 (2023). <https://doi.org/10.1101/2023.04.18.537342>
- 755 54 Zayed, A. A. *et al.* Cryptic and abundant marine viruses at the evolutionary origins of
756 Earth's RNA virome. *Science* **376**, 156-162 (2022).
757 <https://doi.org/10.1126/science.abm5847>
- 758 55 Charon, J., Buchmann, J. P., Sadiq, S. & Holmes, E. C. RdRp-scan: A bioinformatic
759 resource to identify and annotate divergent RNA viruses in metagenomic sequence
760 data. *Virus Evol* **8**, veac082 (2022). <https://doi.org/10.1093/ve/veac082>
- 761 56 Jumper, J. *et al.* Highly accurate protein structure prediction with AlphaFold. *Nature*
762 **596**, 583-589 (2021). <https://doi.org/10.1038/s41586-021-03819-2>
- 763 57 Mirdita, M. *et al.* ColabFold: making protein folding accessible to all. *Nature Methods*
764 **19**, 679-682 (2022). <https://doi.org/10.1038/s41592-022-01488-1>

- 768 58 Li, Z., Jaroszewski, L., Iyer, M., Sedova, M. & Godzik, A. FATCAT 2.0: towards a
769 better understanding of the structural diversity of proteins. *Nucleic Acids Research*
770 **48**, W60-W64 (2020). [https://doi.org:10.1093/nar/gkaa443](https://doi.org/10.1093/nar/gkaa443)
771 59 Marcelino, V. R. *et al.* CCMetagen: comprehensive and accurate identification of
772 eukaryotes and prokaryotes in metagenomic data. *Genome Biol* **21**, 103 (2020).
773 [https://doi.org:10.1186/s13059-020-02014-2](https://doi.org/10.1186/s13059-020-02014-2)
774 60 Clausen, P. T. L. C., Aarestrup, F. M. & Lund, O. Rapid and precise alignment of raw
775 reads against redundant databases with KMA. *BMC Bioinformatics* **19**, 307 (2018).
776 [https://doi.org:10.1186/s12859-018-2336-6](https://doi.org/10.1186/s12859-018-2336-6)
777 61 Cruz-Bustos, T. *et al.* The transcriptome from asexual to sexual in vitro development
778 of *Cystoisospora suis* (Apicomplexa: Coccidia). *Sci Rep* **12**, 5972 (2022).
779 [https://doi.org:10.1038/s41598-022-09714-8](https://doi.org/10.1038/s41598-022-09714-8)
780 62 Palmieri, N. *et al.* The genome of the protozoan parasite *Cystoisospora suis* and a
781 reverse vaccinology approach to identify vaccine candidates. *Int J Parasitol* **47**, 189-
782 202 (2017). [https://doi.org:10.1016/j.ijpara.2016.11.007](https://doi.org/10.1016/j.ijpara.2016.11.007)
783 63 Bushnell, B., Rood, J. & Singer, E. BBMerge - Accurate paired shotgun read merging
784 via overlap. *PLoS One* **12**, e0185056 (2017).
785 [https://doi.org:10.1371/journal.pone.0185056](https://doi.org/10.1371/journal.pone.0185056)
786 64 Buchfink, B., Reuter, K. & Drost, H.-G. Sensitive protein alignments at tree-of-life
787 scale using DIAMOND. *Nature Methods* **18**, 366-368 (2021).
788 [https://doi.org:10.1038/s41592-021-01101-x](https://doi.org/10.1038/s41592-021-01101-x)
789 65 Fauver, J. R. *et al.* Xenosurveillance reflects traditional sampling techniques for the
790 identification of human pathogens: A comparative study in West Africa. *PLoS Negl*
791 *Trop Dis* **12**, e0006348 (2018). [https://doi.org:10.1371/journal.pntd.0006348](https://doi.org/10.1371/journal.pntd.0006348)
792 66 Grubaugh, N. D. *et al.* Xenosurveillance: a novel mosquito-based approach for
793 examining the human-pathogen landscape. *PLoS Negl Trop Dis* **9**, e0003628 (2015).
794 [https://doi.org:10.1371/journal.pntd.0003628](https://doi.org/10.1371/journal.pntd.0003628)
795 67 Shackelton, L. A. & Holmes, E. C. The role of alternative genetic codes in viral
796 evolution and emergence. *J Theor Biol* **254**, 128-134 (2008).
797 [https://doi.org:10.1016/j.jtbi.2008.05.024](https://doi.org/10.1016/j.jtbi.2008.05.024)
798 68 Chen, Y. M. *et al.* RNA viromes from terrestrial sites across China expand
799 environmental viral diversity. *Nat Microbiol* **7**, 1312-1323 (2022).
800 [https://doi.org:10.1038/s41564-022-01180-2](https://doi.org/10.1038/s41564-022-01180-2)
801 69 Venkataraman, S., Prasad, B. & Selvarajan, R. RNA Dependent RNA Polymerases:
802 Insights from Structure, Function and Evolution. *Viruses* **10** (2018).
803 [https://doi.org:10.3390/v10020076](https://doi.org/10.3390/v10020076)
804 70 Martin, M. Cutadapt removes adapter sequences from high-throughput sequencing
805 reads. *2011* **17**, 3 (2011). [https://doi.org:10.14806/ej.17.1.200](https://doi.org/10.14806/ej.17.1.200)
806 71 Andrews, S. *FastQC*, <<https://github.com/s-andrews/FastQC>> (2023).
807 72 Kopylova, E., Noé, L. & Touzet, H. SortMeRNA: fast and accurate filtering of
808 ribosomal RNAs in metatranscriptomic data. *Bioinformatics* **28**, 3211-3217 (2012).
809 [https://doi.org:10.1093/bioinformatics/bts611](https://doi.org/10.1093/bioinformatics/bts611)
810 73 Li, D., Liu, C. M., Luo, R., Sadakane, K. & Lam, T. W. MEGAHIT: an ultra-fast single-
811 node solution for large and complex metagenomics assembly via succinct de Bruijn
812 graph. *Bioinformatics* **31**, 1674-1676 (2015).
813 [https://doi.org:10.1093/bioinformatics/btv033](https://doi.org/10.1093/bioinformatics/btv033)
814 74 Katoh, K. & Standley, D. M. MAFFT multiple sequence alignment software version 7:
815 improvements in performance and usability. *Mol Biol Evol* **30**, 772-780 (2013).
816 [https://doi.org:10.1093/molbev/mst010](https://doi.org/10.1093/molbev/mst010)
817 75 Li, B. & Dewey, C. N. RSEM: accurate transcript quantification from RNA-Seq data
818 with or without a reference genome. *BMC Bioinformatics* **12**, 323 (2011).
819 [https://doi.org:10.1186/1471-2105-12-323](https://doi.org/10.1186/1471-2105-12-323)
820 76 Meng, E. C. *et al.* UCSF ChimeraX: Tools for structure building and analysis. *Protein*
821 *Sci* **32**, e4792 (2023). [https://doi.org:10.1002/pro.4792](https://doi.org/10.1002/pro.4792)

- 822 77 Jones, P. *et al.* InterProScan 5: genome-scale protein function classification.
823 *Bioinformatics* **30**, 1236-1240 (2014). <https://doi.org/10.1093/bioinformatics/btu031>
- 824 78 Kelley, L. A., Mezulis, S., Yates, C. M., Wass, M. N. & Sternberg, M. J. The Phyre2
825 web portal for protein modeling, prediction and analysis. *Nat Protoc* **10**, 845-858
826 (2015). <https://doi.org/10.1038/nprot.2015.053>
- 827 79 Zimmermann, L. *et al.* A Completely Reimplemented MPI Bioinformatics Toolkit with a
828 New HHpred Server at its Core. *Journal of Molecular Biology* **430**, 2237-2243 (2018).
829 [https://doi.org:https://doi.org/10.1016/j.jmb.2017.12.007](https://doi.org/https://doi.org/10.1016/j.jmb.2017.12.007)
- 830 80 van Kempen, M. *et al.* Fast and accurate protein structure search with Foldseek.
831 *Nature Biotechnology* (2023). <https://doi.org/10.1038/s41587-023-01773-0>
- 832 81 Sievers, F. *et al.* Fast, scalable generation of high-quality protein multiple sequence
833 alignments using Clustal Omega. *Mol Syst Biol* **7**, 539 (2011).
834 <https://doi.org/10.1038/msb.2011.75>
- 835 82 Edgar, R. C. Muscle5: High-accuracy alignment ensembles enable unbiased
836 assessments of sequence homology and phylogeny. *Nat Commun* **13**, 6968 (2022).
837 <https://doi.org/10.1038/s41467-022-34630-w>
- 838 83 Capella-Gutiérrez, S., Silla-Martínez, J. M. & Gabaldón, T. trimAl: a tool for
839 automated alignment trimming in large-scale phylogenetic analyses. *Bioinformatics*
840 **25**, 1972-1973 (2009). <https://doi.org/10.1093/bioinformatics/btp348>
- 841 84 Minh, B. Q. *et al.* IQ-TREE 2: New Models and Efficient Methods for Phylogenetic
842 Inference in the Genomic Era. *Mol Biol Evol* **37**, 1530-1534 (2020).
843 <https://doi.org/10.1093/molbev/msaa015>
- 844 85 Yu, G. Using ggtree to Visualize Data on Tree-Like Structures. *Curr Protoc*
845 *Bioinformatics* **69**, e96 (2020). <https://doi.org/10.1002/cpbi.96>
- 846 86 Yu, G., Lam, T. T., Zhu, H. & Guan, Y. Two Methods for Mapping and Visualizing
847 Associated Data on Phylogeny Using Ggtree. *Mol Biol Evol* **35**, 3041-3043 (2018).
848 <https://doi.org/10.1093/molbev/msy194>
- 849